

THRUST STAND FOR APPLIED-FIELD MPD THRUSTERS

IEPC-2005-215

*Presented at the 29th International Electric Propulsion Conference, Princeton University,
October 31 – November 4, 2005*

James H. Gilland*
Ohio Aerospace Institute, Brookpark, OH, 44142, USA

Mitchell L. R. Walker†
Georgia Institute of Technology, Atlanta, GA, 30332, USA

Eric J. Pencil‡
NASA Glenn Research Center, Cleveland, OH 44135, USA

Abstract: The Magnetoplasmadynamic (MPD) thruster has the potential for operating at both high specific impulse (I_{sp}) and high power. As a high power concept, the performance and lifetime of these devices are not yet known well enough to allow an optimized design. The NASA Glenn Research Center (GRC) team is investigating the performance of self- and applied-field MPD thrusters using non-condensable propellants. A quasi-steady thruster test facility, capable of operation up to 10 MW_e at mass flow rates of 0.25 – 1 g/s, has been constructed, including an inverted pendulum thrust stand. The self-field performance of a “benchmark” thruster design using argon propellant has been measured previously. Extension of the performance database to include applied-field effects, however, has been hampered by the interaction of the initial magnetic field transient with the vacuum facility. The thrust stand has been revamped to allow for active damping of the magnetic field perturbation prior to the discharge. The improvement in thrust stand operation with an applied-field is described.

Nomenclature

GRC	=	Glenn Research Center
I_{sp}	=	Specific Impulse (u_e/g_0), seconds
J	=	Current, kiloamperes
LVDT	=	Linear variable Displacement Transducer
\dot{m}	=	Propellant mass flow rate, g/s
MW _e	=	Megawatts of electrical power
T	=	Tesla
V	=	MPD Voltage

I. Introduction

Mission studies for planetary (and beyond) missions have repeatedly shown the benefits of multimegawatt electric propulsion to decrease trip time or increase payload mass.^{1,2} Currently, no single thruster candidate has been

* Senior Scientist, Space Science, Propulsion, and Communications Team, james.h.gilland@nasa.gov.

† Assistant Professor, School of Aerospace Engineering, mitchell.walker@ae.gatech.edu.

‡ Research Engineer, Electric Propulsion Branch, eric.j.pencil@nasa.gov.

identified that will simultaneously meet the mission requirements of power level (1-5 MWe/thruster), specific impulse (2 – 10 ks), and efficiency (> 50%).³ One candidate is the Magnetoplasmadynamic (MPD) thruster, which has demonstrated the capability to operate at relevant power levels and specific impulse.⁴ As with other high power thruster concepts, MPD thruster development has lagged behind lower power concepts. This has been due in part to the lack of available space power to take advantage of the MPD thruster's unique power handling capability, and in part to the difficulty of steady state testing at MWe power levels. While the MPD thruster has in fact demonstrated MWe operation and mission-relevant Isp's, the concept still requires improvement in efficiency and lifetime. Although both requirements must ultimately be met for successful application to exploration missions, MPD thruster performance can be examined and improved through cost effective pulsed operation in low cost vacuum facilities, whereas lifetime assessment and demonstration requires extended operation over 1000's of hours.⁵

MPD performance has been found to depend on a wide parameter space: thruster geometry⁶, propellant⁷, propellant injection sites^{8,9}, and applied-field strength and shape¹⁰. A range of theoretical and empirical models exist to explain the effects of these variables^{11,12,13}; however, a significantly broad data base of MPD thruster performance and behavior over all parameters does not exist to test all of the model predictions¹⁴. To address this need, NASA GRC has developed a facility and program aimed at expanding the experimental data base and benchmarking model predictions. The scope of testing covers non-condensable propellants such as argon or hydrogen, self- and applied-field thrusters, and power levels from 100's of kWe to MWe. The focus on performance allows experiments to be conducted in a pulsed mode; this mode of operation precludes lifetime assessment due to the drastic difference in electrode erosion between pulsed and steady state operation.¹⁵

II. Facility and Previous Thrust Stand

The current facility (shown in Fig. 1) consists of a pulse forming network, high voltage power supply to energize the network, mass injection system, applied field magnet coil, magnet power supply, and control and acquisition system. All subsystems are currently operational. The facility has been described in detail in previous reports⁵. Only the pertinent details of the facility operation as it pertains to the applied-field thrust measurement method will be described.

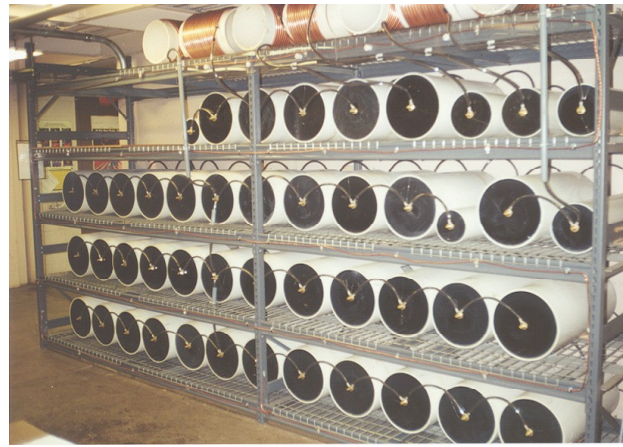


Figure 1. MPD thruster testing facility and pulsed power supply.

A. Pulsed Power System

The pulse forming network uses 46 capacitors and 7 inductors arranged in a 7-element Guillemin circuit. Each capacitor is rated for 10-kVDC. The system is connected to the thruster electrodes through a solid-state thyristor rated for 15-kV and 50-kA peak current. The system is charged to kV levels to initiate breakdown across the thruster electrodes. The design pulse length is on the order of 2 ms. Recent self-field operation with the NASA GRC benchmark thruster has ranged from 3 to 10 kA at 0.75 g/s. An example current pulse is shown in Figure 2.

B. Mass Injection System

The mass injection system is external to the vacuum facility. It consists of a propellant plenum, fast acting pneumatic valve (powered by building shop air), solenoid valve to activate the fast acting valve, and pressure gauges in the plenum and at the entrance to the thruster. The cylindrical plenum chamber is constructed of stainless steel, with an interior volume of $2.5 \times 10^{-2} \text{ m}^3$. The system has been operated at mass flow rates up to 0.75 g/s. A plenum pressure of 1200 Torr is required for 0.75 g/s in the current system. Because of the long flow path between the valve and the thruster chamber, a 180 ms period is required for the flow to reach equilibrium before the discharge is initiated. A representation of the pressure trace measured at a point immediately before flow enters the thruster is shown in Fig. 3 (the discharge would occur at approximately $t = 0$). The extended mass flow equilibration time means that there is an extended period of cold flow thrust prior to initiation of the discharge.

C. Applied Field Coil and Power Supply

To test the effects of applied axial and radial fields, the NASA GRC thruster is mounted coaxially with an uncooled magnet consisting of insulated 4-AWG copper cabling wound on a 0.2 m (8") OD pvc pipe. The insulated cabling is continuously wound in 7 layers, with 18 turns per layer. Because the magnet is not cooled, both the maximum current and the period of operation are limited; however, the higher field strength that can be achieved through the more compact wrapping of uncooled coils outweighs these disadvantages.

Power is supplied by a 50-kW constant-current arc welder, capable of delivering up to 1000 A to the magnet. The measured axial magnetic field strength at the center of the magnet coil is roughly $5 \times 10^{-4} \text{ T/A}$, while at the end of the coil the axial field along the centerline is approximately $3.3 \times 10^{-4} \text{ T/A}$. The magnet is operated over a 4.5 second time scale. Magnet is the limiting factor in pulse rate, to allow the magnet coil to cool between shots. As will be described in Section III, the extended magnet pulse length is used to minimize interaction of the magnet with the thrust stand.

D. Control and Acquisition System

Thruster operation is determined by the constraints imposed by the mass injection system and the applied field magnet. A custom control board is used to ensure the proper timing of magnet turn-on, mass injection, and discharge switching. The experimental firing sequence proceeds in sequential order and is shown graphically in Fig. 4:

1. Magnet power is turned on for 4.5 seconds.
2. Mass injection valve opens for an approximately 230 millisecond pulse.
3. The thruster switch fires 180 milliseconds after mass flow starts.
4. Mass injection and magnet turn off.

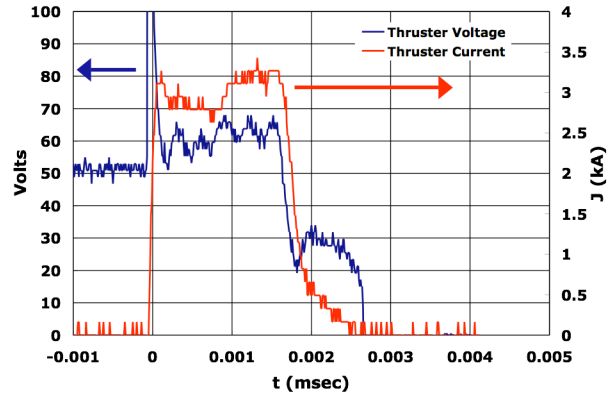


Figure 2. Sample 3 kA current pulse and MPD thruster discharge voltage for self-field thruster operating at 0.75 g/s Argon.

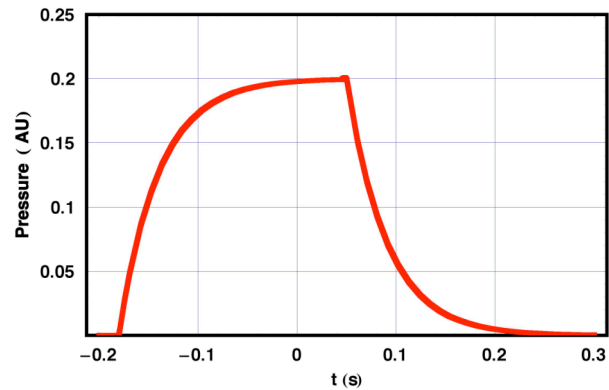


Figure 3. Representative pressure pulse shape at thruster inlet.

	Time (s)				
	1	2	3	4	5
Discharge					
Gas Flow On					
Magnet On					

Figure 4. Timeline of MPD thruster firing process.

The delay between the start of mass injection and thruster firing can be varied through varying changing resistor settings in the circuit.

Thruster voltage is measured at the anode and cathode through a voltage divider circuit. The difference between these two voltages is recorded as the thruster voltage. Similarly, current in and out of the thruster is measured using two current transformers. The capability for reading both directions of current flow is used to verify that the discharge is flowing between the thruster electrodes rather than arcing to ground through some other path. Both current and voltage are recorded on digital oscilloscopes, and downloaded to PC as data files for further analysis later.

E. Applied Field Impulse and Previous Thrust Stand

The MPD thrust stands, past and present, are based on an inverted pendulum concept that has been applied to a variety of electric thrusters.¹⁶ The thruster and magnetic field coil are mounted on a support platform resting on 4 flexure supports that allow the thruster/coil assembly to oscillate freely over a span of several centimeters. The spring constant of the flexures and the mass of the thruster determine the period of motion for the pendulum. In this case, the period is on the order of 1.4 seconds. Because of the long period, the thrust stand response is related to the total impulse delivered, rather than the instantaneous thrust. The thrust stand is sensitive enough to respond to both the cold gas flow through the thruster as well as the thrust from the MPD discharge.

Prior to this work, thrust stand motion was measured using a dynamic load cell attached to the rigid base of the thrust stand. Because of systematic vibrational noise, the pendulum was isolated from rigid contact with the load cell by using repulsive permanent magnets. This approach, in conjunction with detailed calibration, was effective for self-field measurements.⁴ However, when the applied field coil was activated during thruster tests for applied field measurements, the inductive interaction between the applied-field coil start-up and the conducting tank door was found to produce an impulse comparable to the cold thrust response. An additional concern with previous permanent magnet coupling method was the interaction of the applied field with the permanent magnets. The thrust stand response to a magnet coil transient at a current of 300 A, and the separately measured cold gas response at a mass flow rate of 0.75 g/s, are shown relative to each other in amplitude and time in Fig 4. After some unsuccessful attempts at shielding these interactions, the necessity of actively damping this premature motion became evident. Active damping required a feedback circuit, which was not possible with the load cell. The thrust stand was therefore modified in 2005 to use a linear variable displacement transducer (LVDT) in concert with feedback damping system.

III. Revised Applied-field Thrust Stand

A. LVDT Stand Calibration

Figure 6 shows the GRC benchmark MPD thruster mounted on the revised inverted-pendulum thrust stand. An electromechanical active damping coil has been installed to eliminate the oscillation created by energizing the applied-field magnet before firing. The damper is on during the magnet start up and turned off after 3 seconds, approximately 1 second prior to initiation of the mass flow and discharge. This thrust stand has been calibrated in the same manner used for the load cell

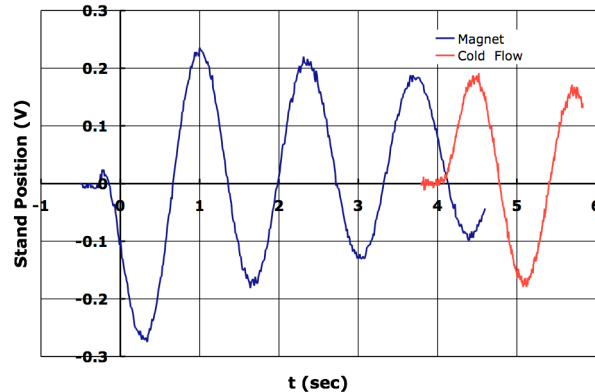


Figure 5. Comparison of undamped magnetic field transient with a 0.75 g/s cold pulse thrust stand response.

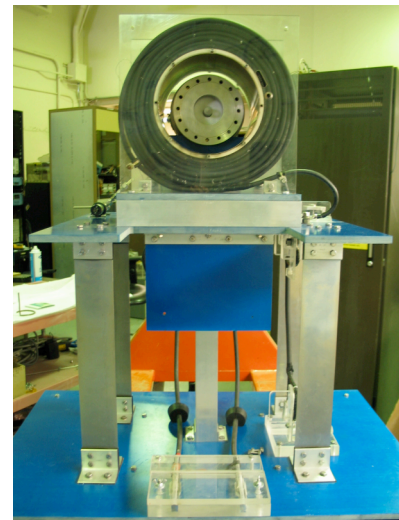


Figure 6. LVDT thrust stand with GRC benchmark thruster and applied field coil.

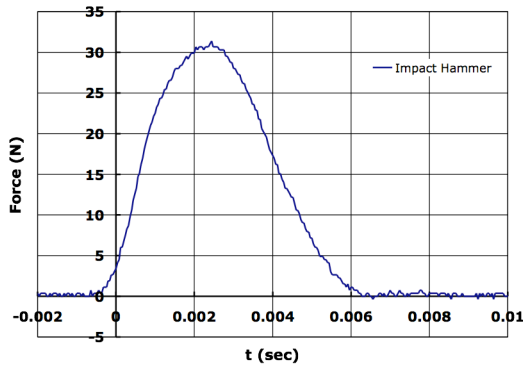


Figure 7. Impact hammer force signal (note millisecond time scale).

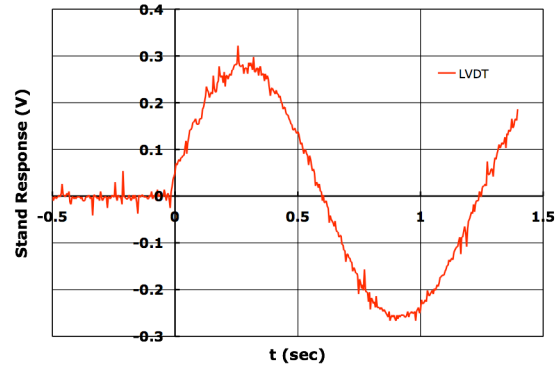


Figure 8. Thrust stand displacement response to impulse in Fig. 7, as measured by LVDT.

measurement, using the measured impulse from an electrical impact hammer. The hammer provides impact forces and millisecond time scales comparable to those expected over the full range of thruster operation.⁵ A dynamic load cell like the one used on the thrust stand is installed on the thruster, in front of the cathode tip. The hammer force versus time curve is integrated to give the impulse delivered to the thruster. Simultaneously, the thrust stand displacement signal for each hammer impulse is recorded. The thrust stand natural period is approximately 1.4 seconds. The integral of one-half cycle of thrust stand oscillation and the maximum deflection after impact correlate directly to the impulse delivered to the thrust stand. The half-cycle integral is used in measurement and calibration to filter out some of the higher frequency noise that is seen on the LVDT. A sample hammer force curve and the corresponding stand displacement response are shown in Fig. 7 and 8. The calibration curve created from this technique is used to determine the thrust created by the thruster. The calibration results for the LVDT stand are shown in Fig. 9. The horizontal axis is the half-period integral of the LVDT signal. The vertical axis is the thrust value for an impulse pulse length of 2 milliseconds, corresponding to thruster operation.

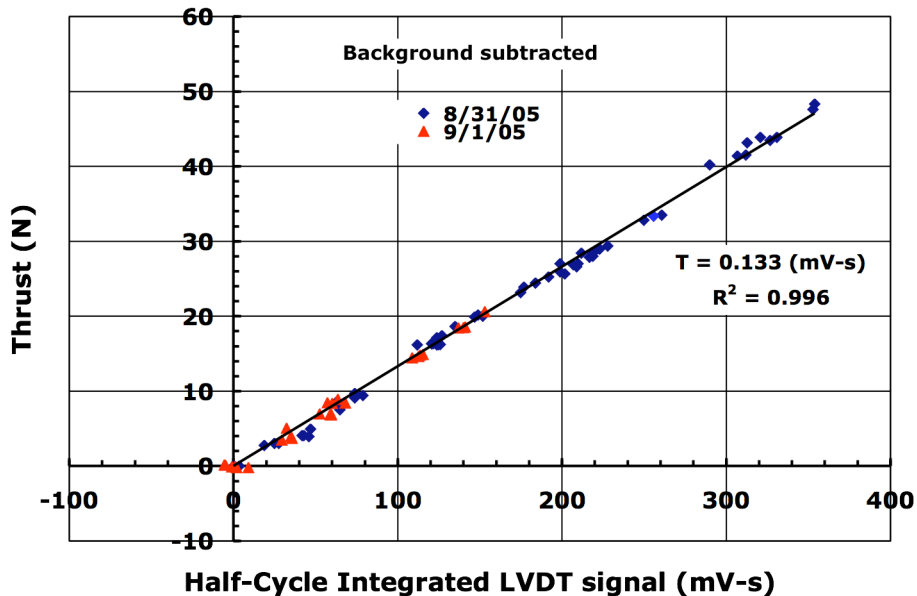


Figure 9. LVDT Thrust stand calibration using impact hammer.

B. Initial Self-Field Thrust Measurements

The new thrust measurement approach was first tested using the GRC thruster operating in self-field mode. The thruster was operated at 0.75 g/s flow rate at currents from 3 to 10 kA. The self-field thrust was determined by measuring the response the cold flow and thrust, and then subtracting the cold flow contribution. The net thrust measured at 0.75 g/s using the LVDT stand is shown for a range of current levels in Fig. 10. Also shown are the self-field measurements taken previously using the load cell thrust stand. Above 5 kA, the thrust measurements show good agreement over their common region of operation. Low thrust values (currents below 5 kA) have greater scatter using either method. This uncertainty at the lower thrust levels stems from the relative magnitudes of the cold flow impulse and the thruster impulse. Although the cold flow thrust is relatively small, the cold flow operating time before the discharge is 180 ms, while the thrust impulse itself is only 2 ms. The cold flow impulse is therefore comparable to or greater than the MPD thrust at low currents.

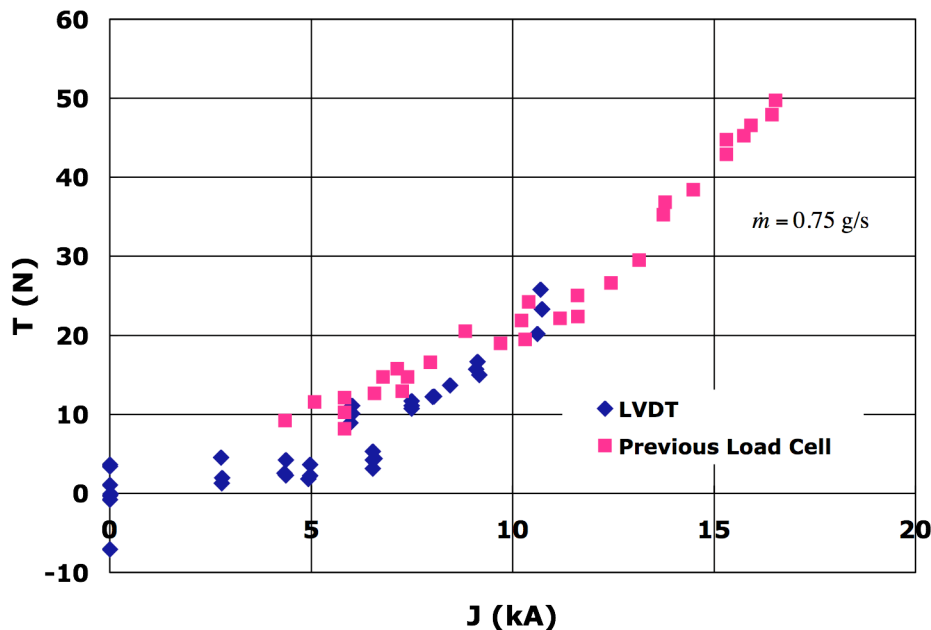


Figure 10. Self-field thrust measurements at 0.75 g/s compared to previous tests.

C. Operation with Damper

Although operation of the GRC MPD thruster in applied-field mode was not possible for this report, preliminary tests of the damping circuit with the applied field have been conducted. The results are shown in Fig. 11 for a 300 A current pulse to the applied field magnet, corresponding to a centerline magnetic field of 0.15 T. The damped signals are compared to the undamped signal, and to a mass flow pulse shown at the same relative time as it would occur in the operation of the thruster. The damper was used in two ways for this test: 1.) operating continuously throughout the magnet pulse, and 2.) operating for the first 3 seconds of the magnet operation, then shut off manually. Use of the damper results in reduction of the applied-field-induced oscillations within 2 periods of the oscillation. A slight oscillation after the damper is shut off can be seen; however, the magnitude is significantly lower than the undamped oscillation, and should allow thrust measurements to be made. The damping force could also be increased to damp the motion sooner, but this would require an increase in the power supplied to the coil. It could also lead to higher amplitude oscillations when the damper is turned off. The offset in the zero level of the thrust stand does not impact the measurement, as the change in position, not the absolute position, relates to the impulse.

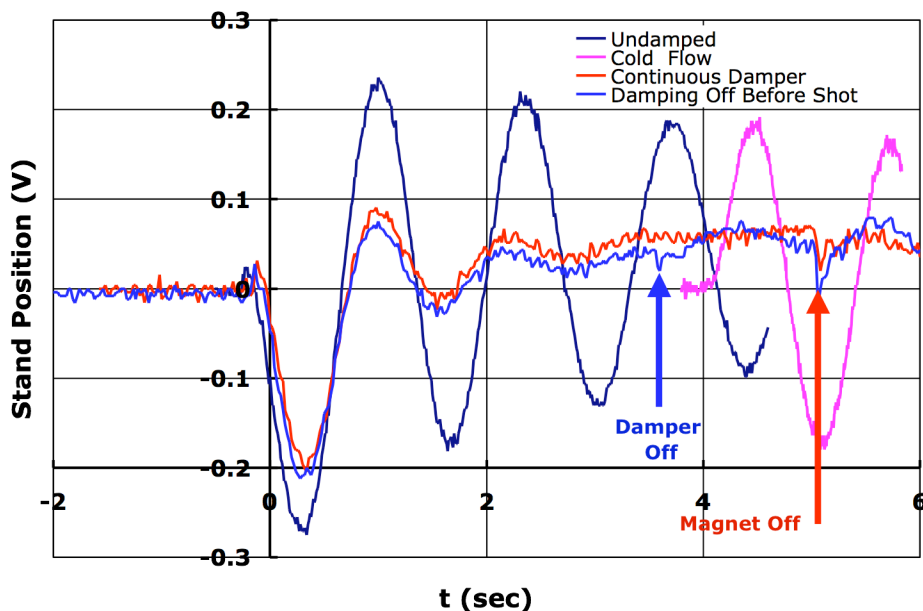


Figure 11. Comparison of thrust stand response to magnet force with and without damper.

IV. Summary

The GRC MPD thrust stand has been upgraded to allow accurate thrust measurement of applied-field MPD thrusters. The new LVDT system with an incorporated active damping system allows for the reduction or elimination of additional stand motion caused by the applied field coil startup. This reconfigured thrust stand has been calibrated and used to measure self-field thruster performance. Sample self-field thrust measurements are in good agreement with those measured using the previous load cell method. The thrust stand has also been tested during operation with the applied field coil, but without discharge, and found to effectively damp out the field coil perturbations prior to the discharge. This shall allow the GRC MPD performance database to include the effect of applied fields.

Acknowledgements

The authors thank Mr. Thomas Haag for his help and advice in redesigning and testing the LVDT thrust stand. The authors also wish to acknowledge the invaluable aid of Mr. Donald Fong in maintaining the accuracy of the MPD test control system, and Mr. James Coy and Ms. Donna Neville for their assistance and patience in construction and testing of the LVDT thrust stand.

References

- ¹ Nock, K. T., "TAU - A mission to a thousand astronomical units," AIAA-1987-1049, 19th International Electric Propulsion Conference, Colorado Springs, CO, May 11-13, 1987.
- ² Hack, K. J. et al., "Evolutionary Use of Nuclear Electric Propulsion," AIAA-90-3821, Sept. 1990.
- ³ Gilland, J., "NEP Mission Sensitivities to System Performance," NASA CR-189059, Dec. 1991.
- ⁴ Lapointe, M., Pencil, E., and Strzempkowski, E., "High Power MPD Thruster Performance Measurements," AIAA-2004-3467, July, 2004.
- ⁵ Lapointe, M. and Mikellides, P., "High Power MPD Thruster Development at the NASA Glenn Research Center," AIAA-2001-3499, July, 2001.
- ⁶ King, D. Q., *Magnetoplasmdynamic Channel Flow for Design of Coaxial MPD Thrusters*, Ph.D. Thesis, Princeton University, Dec. 1981.
- ⁷ Polk, J. E., and T.J. Pivrotto. "Alkalimetal propellants for MPD thrusters," AIAA-91-3572, Oct. 1991.

-
- ⁸ Merfeld, D. J., A.J. Kelly, and R.G. Jahn, "MPDT performance: Propellant injection and species effects." 18th International Electric Propulsion Conference, Alexandria, VA, AIAA-85-2022, Oct. 1985.
- ⁹ Paganucci, F., Rossetti, P., Andrenucci, M., Tikhonov, V., and Obukhov, V. A., "Performance of an applied-field MPD thruster with a pre-ionization chamber," 28th International Electric Propulsion Conference, Toulouse, France, IEPC-03-302, Mar. 2003.
- ¹⁰ Tikhonov, V. B., N.N. Antropov, G.A. Dyakonov, V.A. Obukhov, F. Paganucci, P. Rossetti, M. Andrenucci, "Investigation on a new type of MPD Thruster," *Proc. of the 27th EPS Conf. on Contr. Fusion and Plasma Phys.*, Budapest, Hungary, **24B**, June, 2000.
- ¹¹ Kagaya, Y., H. Tahara, and T. Yoshikawa, "Effect of applied magnetic nozzle in a quasi-steady MPD thruster," 28th International Electric Propulsion Conference, Toulouse, France, IEPC-03-031, Mar. 2003.
- ¹² Tikhonov, V. B. et al., "Research of Plasma Acceleration Processes in Self-Field and Applied Magnetic Field Thrusters," in *Proc. 23rd International Electric Propulsion Conference*, IEPC-93-076, Seattle, WA, 13-16 September 1993.
- ¹³ Mikellides, P., and Turchi, P. "Applied-Field Magnetoplasma-dynamic Thrusters, Part 2: Analytic Expressions for Thrust and Voltage", *J. Propulsion and Power*, 16 (5), Sept-Oct 2000, pp. 894-901.
- ¹⁴ Gilland, J. H., "System-Level Models of Self- and Applied-Field MPD Thrusters," 40th Joint Propulsion Conference, AIAA-2004-3470, Fort Lauderdale, FL, July, 2004.
- ¹⁵ Polk, J., A. Kelly, R. Jahn, H. Kurtz, M. Auweter-Kurtz, and H. O. Schrade, "Mechanisms of Hot Cathode Erosion in Plasma Thrusters," AIAA-90-2673, Orlando, Florida, July 1990.
- ¹⁶ Haag, T.W., "Thrust stand for pulsed plasma thrusters," *Review of Scientific Instruments*, Vol. 68, 1997, pp. 2060-2067.